Photo-conversion bonding mechanism in ruthenium sulfur dioxide linkage photo-isomers revealed by *in-situ* diffraction

Sven O. Sylvester, Jacqueline M. Cole*, Paul G. Waddell

*To whom correspondence should be addressed. Email: jmc61@cam.ac.uk

Supplementary Information

Experimental Section

trans-tetraaminepyrdine(sulphur dioxide)ruthenium(II) chloro hydrate (1)

trans-$[Ru(NH_3)_4SO_2Cl]Cl$ (5 mg, 16 μmol) prepared by literature methods,[1] was dissolved in a sodium carbonate solution (700 μL, 1 M). Pyridine (400 μL) was added to the solution and after 5 minutes HCl (400 μL, 32%) was added. Fine bricklike pink crystals appeared overnight which were isolated through vacuum filtration and washed with methanol. A small crystal suitable for X-ray analysis was selected from the solid.

trans-tetraamine(3-chloropyrdine)(sulphur dioxide)ruthenium(II) chloro hydrate (2)

trans-$[Ru(NH_3)_4SO_2Cl]Cl$ (12 mg, 40 μmol) was dissolved in H_2O (500 μL) and heated at 60˚C for 2 minutes and 3-chloropyridine (400 μL, 98%) was subsequently added. The solution was phase separated and HCl (100 μL, 32%) was added to the aqueous phase. The solution was left for 2 h and orange needle-like crystals were isolated through vacuum filtration and washed with ethanol and acetone. A small crystal suitable for X-ray analysis was selected from the solid.

trans-tetraamine(4-chloropyrdine)(sulphur dioxide)ruthenium(II) chloro hydrate (3)

trans-$[Ru(NH_3)_4SO_2Cl]Cl$ (5 mg, 16 μmol) was dissolved in a sodium carbonate solution (700 μL, 1 M). 4-chloropyridine (400 μL) was added to the solution and after 5 minutes HCl (400 μL, 32%) was added. Fine bricklike pink crystals appeared overnight which were isolated through vacuum filtration and washed with methanol. A small crystal suitable for X-ray analysis was selected from the solid.

Refinement Details:

The atomic displacement parameters were refined anisotropically for all non-hydrogen atoms, unless otherwise stated. The hydrogen atoms were initially placed in idealised positions for the ammine and aromatic H atoms with $U_{iso}(H) = 1.5U_{eq}(N)$ and $1.5U_{eq}(C)$ respectively. The H atoms on the water of crystallisation were located from the electron density Fourier difference map and refined freely. After photo-excitation all non-H atoms present in the isomerisation were located through the Fourier difference maps. The ADPs of the SO_2 photo-excited isomers of **1** were constrained to the corresponding value of the GS (SIMU instruction in SHELX[2]) and no restraints of constraints were used for **2** and **3**.

Spectrum of Thor-labs LED Light

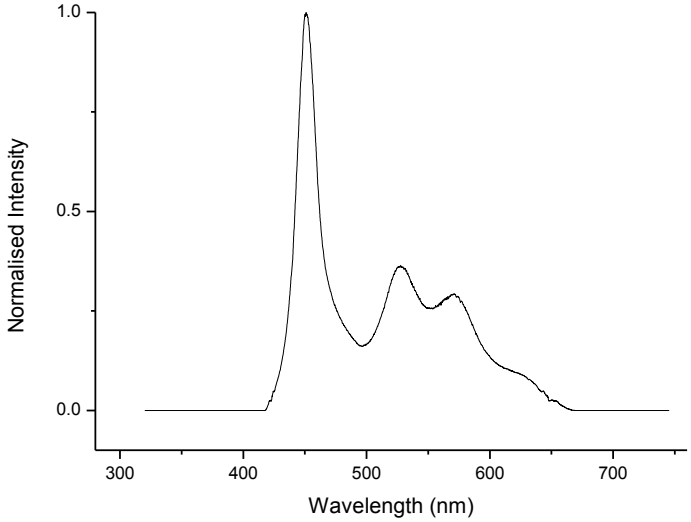

Figure S1: The full spectrum of the Thor-Labs Cold white LED used for photo-excitation.

Traditional First- and Second-Order Kinetics

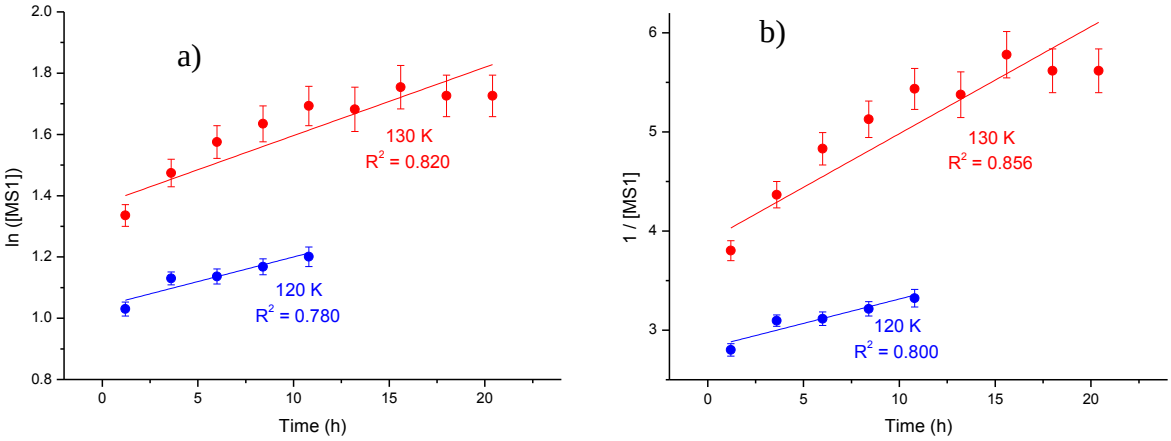

Chart S1: Data from **1** fitted to traditional first-order (a) and second-order (b) kinetics. The high R^2 values suggest that this model doesn't reflect the kinetics.

Reproducibility of MS1 Decay Kinetics

The kinetic experiment on **1** was repeated on a different crystal to determine the reproducibility of the decay kinetics. The crystal, included in the paper (**1a)**, was 0.47 x 0.10 x 0.13 mm in size and the new crystal (**1b**) was 0.28 x 0.12 x 0.13 mm. A photocrystallographic experiment was conducted on **1b** using identical irradiation parameters as on **1a**. The temperature profile for this experiment was slightly varied, with measurements at 100 K, 120 K and 140 K. Immediately after excitation (at 100 K) the ground state occupancies were within error of each other, showing that there was a uniform amount of total isomerisation between the different crystals (Chart S2). There was a ~5% difference in occupancies between the MS1 and MS2 geometries for the different crystals (MS1 = 39.5(9)% and 44.8(7)%, MS2 = 16(1)% and 13.3(9)% for **1a** and **1b** respectively). These differences can be accounted for by experimental variability in photocrystallographic experiments which has not been systematically analysed, for example the effects of crystal size and the reproducibility error of focussing the irradiating light by hand.

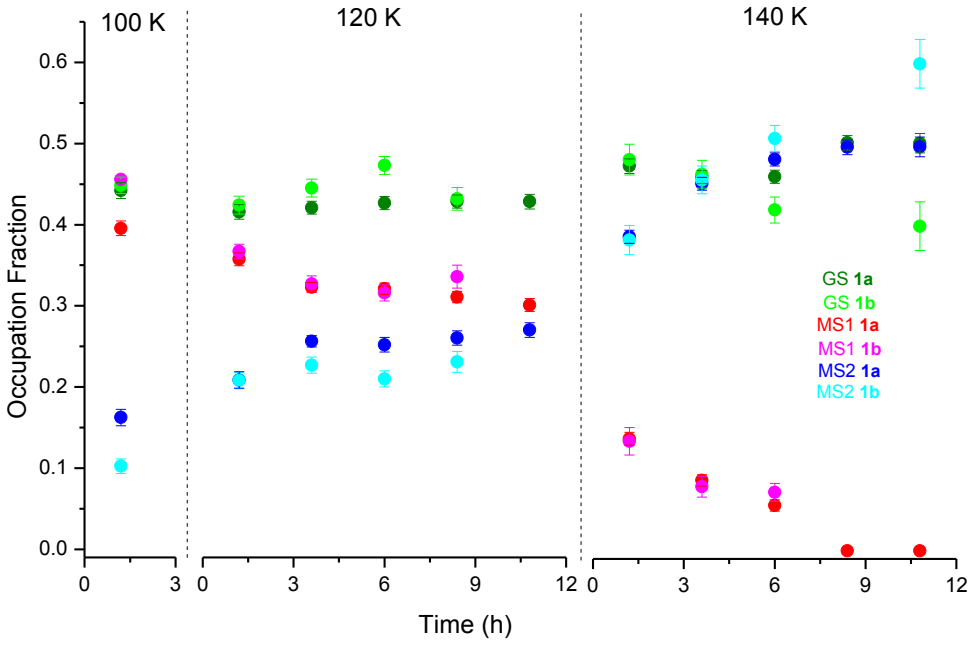

Chart S2: the decay of the MS1 geometry into the MS2 geometry over time at 120 K and 140 K. Each data point reflects a full diffraction experiment. Each data point represents a full diffraction experiment and its time is attributed to the midpoint of the relevant data collection. The time was re-started at each temperature change represent by the dotted lines.

When the temperature was raised to 120 K, the **1a** and **1b** data showed similar trends, with approximately 10% of the MS1 geometry decaying into the MS2 geometry, with both GS geometries remaining constant within experimental error. There is large agreement in the MS1 geometry with the data for **1a** and **1b** within error of each other, and the MS2 geometries are also similar with an occupational fraction difference of less than 3% for all data.

The temperature profile for these two experiments was then changed, with crystal **1a** being heated to 130 K and held there for 19.2 h before being heated to 140 K as opposed to **1b** whose temperature was immediately raised to 140 K. Even though **1a** had gone through a stepwise decay at 130 K with the MS1 occupation dropping to 17.4(3)%, the MS1 occupancy

of **1a** and **1b** at 140 K were within experimental error. This suggests that the decay of the MS1 geometry into the MS2 geometry is purely temperature dependent, with the previous occupancies of the different geometries having little effect on the new occupancy immediately after the temperature increase.

Induced Strain Under High MS2 Isomerisation

In crystal **1b**, when the temperature was initially raised to 120 K, the Bragg spots that were clearly defined at 100 K became elongated and the 2-D diffraction images began to show rings that resemble those of a powder diffraction pattern. This observation is a more extreme version of that seen in previous experiments on the $[Ru(NH_3)_4SO_2H_2O]Tos_2$ complex and which was contributed to the onset of crystal lattice strain.[3] This effect was not present in crystal **1a** which might be attributed to a larger crystal being able to withstand the strain of large MS2 isomerisation, or possibly other microscopic effects such as grain boundaries and dislocations within the crystal.

To examine this strain, the steric interactions can be visualised using Hirshfeld surfaces of the observed excited state geometries. These 3-D isosurfaces were plotted using CrystalExplorer 2.1[4] which partitions the crystal based on the Hirshfeld method which in turn reflects the intermolecular interactions of neighbouring atoms (Figure S1). The three different SO_2 geometries for **1b** allow one to judge if photo-induced crystallographic strain is the likely origin of these diffraction features. Hirschfeld surfaces for the ground state show little positive isoenergy around the SO_2 moiety, with no closest neighbours lower than the sum of the idealised van der Waals radii. Upon photo-isomerisation, the free oxygen of the SO_2 moiety in both the MS1 and MS2 geometries move closer to neighbouring ammine groups thereby inducing crystallographic strain. The closest approach for the free oxygen to the ammine hydrogen reduces from 2.88(4) Å in the GS, to 2.62(2) Å for MS1 and 2.13(4) Å

for MS2, *c.f.* the sum of van der Waals radii of O and H: 2.72 Å. After the initial photo-excitation there is a large amount (44.5(7)%) of the SO_2 in the MS1 geometry with only 13.2(9)% MS2 geometry; however as the decay of the MS1 to MS2 state occurs with the increase in temperature, the amount of internal crystallographic strain increases. Although this strain severely compromises the homogeneity of the diffraction patterns, the crystal is able to relax back from such a large photo-excitation of 60(3)% into the ground state (at room temperature) with no residual evidence of strain or internal crystal cracking.

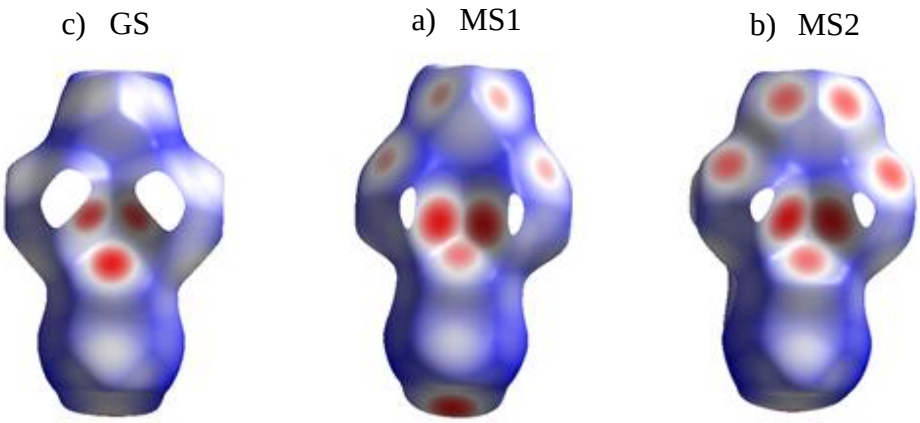

Figure S2: Hirschfeld surfaces for the three different SO_2 geometries in **1b**. The red regions show a positive isoenergy (abnormally close atomic contact), in white regions there is neutral isoenergy, and blue regions display negative isoenergy. The progression of O_{free} towards the ammine hydrogen is evident in the comparison of the GS to MS1 to MS2, which in turn introduces crystallographic strain.

Fourier Difference Maps

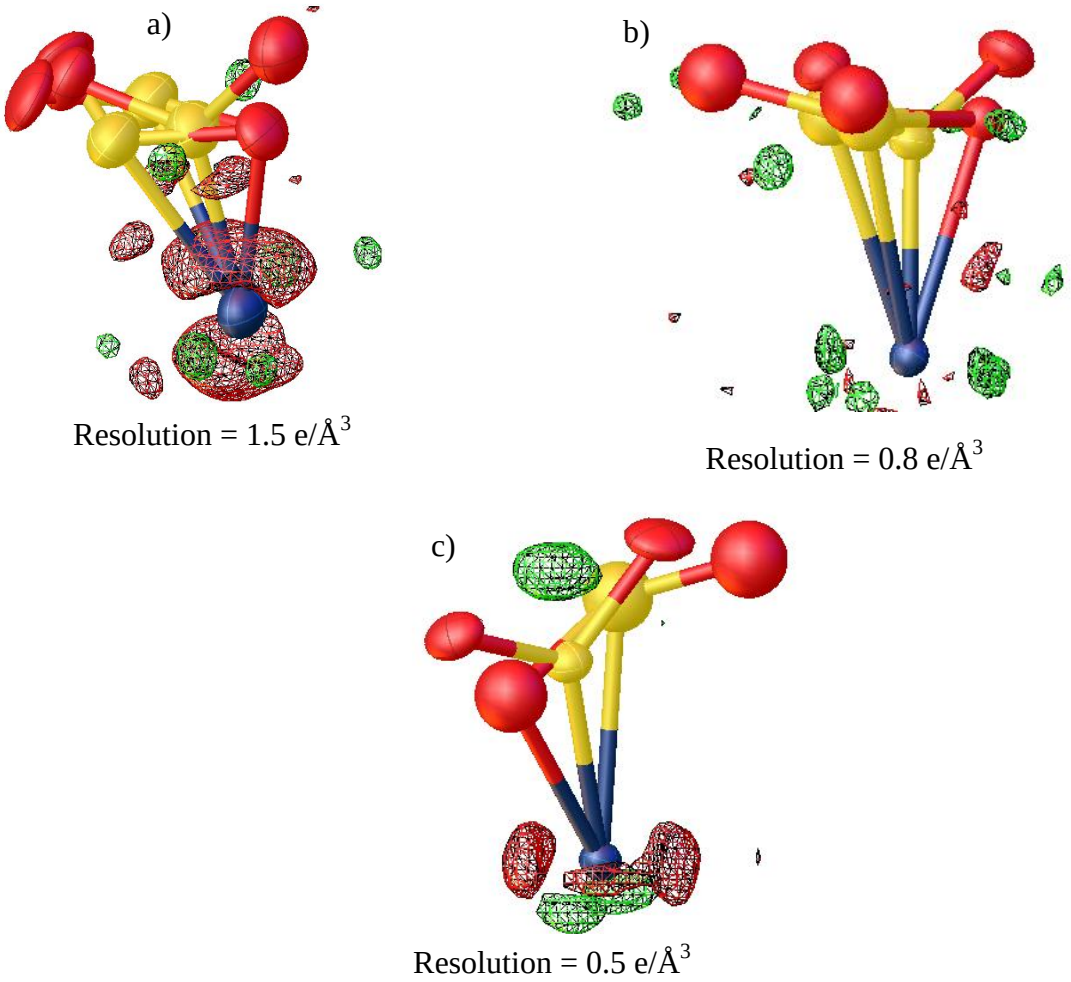

Figure S3: A 3D electron density map imaged using OLEX. The green wire frame represents areas of positive electron density and the red represents areas of negative electron density. The yellow atoms represent sulphur, the red atoms represent oxygen and the blue represents ruthenium. a) **1** after 10 h at 140 K which shows no excess electron density around the MS1 geometry; b) **2** which shows no excess electron density around the MS1 geometry at 100 K; c) **3** which shows a positive electron density around the position of the S atom in the MS1 geometry, however when this was introduced into the model, there was a population of ~3 % and it was not possible to resolve either of the oxygen atoms. This suggests that there might be trace amounts of this geometry, however it is not possible to determine this using a lab X-ray source.

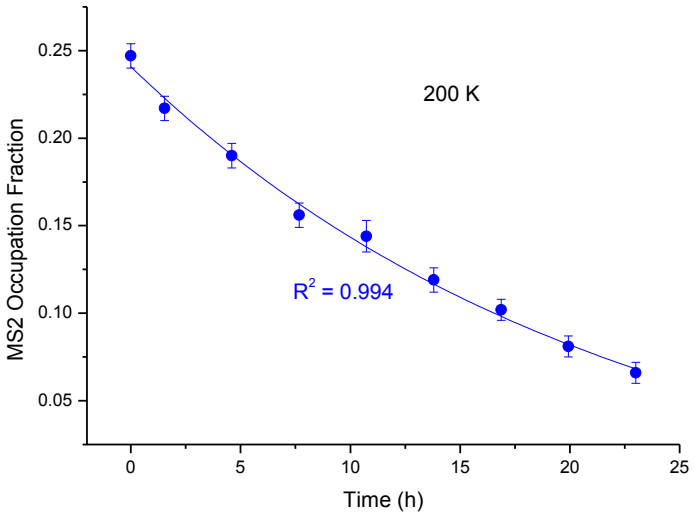

Chart S3: Decay of the MS2 geometry into the GS geometry for **3** showing all 8 data points at 200 K.

Selected Crystallographic Information

Table S1: Crystallographic details for data collected before and after irradiation.

	1 (GS)	**1 (MS1 + MS2)**	**2 (GS)**	**2 (MS2)**	**3 (GS)**	**3 (MS2)**
Crystal Colour/shape	Pink Bricks	Green Brick	Orange Needles	Green Needle	Pink Bricks	Green Brick
Crystal system	Orthorhombic	Orthorhombic	Orthorhombic	Orthorhombic	Monoclinic	Monoclinic
Space group	Pmcn	Pmcn	Pmcn	Pmcn	$P2_1$	$P2_1$
a	6.695 (2)	6.979 (3)	6.858(2)	6.885 (3)	7.129 (2)	7.159 (4)
b	9.636 (3)	9.779 (5)	9.751(4)	9.756 (3)	10.625 (3)	10.674 (6)
c	21.490 (7)	21.672 (5)	23.565(8)	23.372 (8)	9.959 (3)	9.616 (6)
α	90	90	90	90	90	90
β	90	90	90	90	91.675 (3)	91.604 (9)
γ	90	90	90	90	90	90
Z	4	4	4	4	2	2
T (K)	100(2)	100(2)	100(2)	100(2)	100(2)	100(2)
R1 (observed Data)	0.0423	0.0569	0.0572	0.0523	0.0461	0.0499
wR2	0.1289	0.1459	0.1304	0.1174	0.1180	0.1120
Goodness of Fit	1.13	0.850	1.14	1.138	1.06	1.06
Unique Reflections	2477	2686	2924	2857	3636	4687
Number of Parameters	103	130	109	121	172	184

Table S2: Selected bond lengths and angles for the different SO_2 photo-isomer geometries.

	1 (GS)	**1 (MS1)**	**1 (MS2)**	**2 (GS)**	**2 (MS2)**	**3 (GS)**	**3 (MS2)**
Ru-S	2.107 (1)	-	2.55 (2)	2.108 (1)	2.55 (3)	2.107 (1)	2.50 (2)
$Ru\text{-}O_{bound}$	-	1.913 (16)	2.25 (8)	-	2.41 (4)	-	2.13 (4)
$O_{bound}\text{-}S$	1.445 (3)	1.503 (15)	1.61 (9)	1.437 (3)	1.82 (5)	1.441 (5)	1.62 (6)
$S\text{-}O_{free}$	1.453 (3)	1.465 (22)	1.51 (4)	1.449 (3)	1.55 (8)	1.451 (5)	1.34 (5)
$Ru\text{-}N_{pyr}$	2.115 (3)	2.0813 (5)	2.0813 (5)	2.131 (3)	2.120 (4)	2.123 (4)	2.133 (4)
$N_{pyr}\text{-}Ru\text{-}S$	178.86 (11)	-	155.3 (6)	178.75 (8)	160.4 (5)	178.52 (10)	160.4 (4)
$N_{pyr}\text{-}Ru\text{-}O_{bound}$	-	165.2 (5)	165.2 (2)	-	156.2 (9)	-	159.6 (15)
O-S-O	114.80 (20)	114.8 (11)	131.3 (26)	115.45 (18)	117.0 (31)	115.35 (25)	118.1 (27)

References

(1) Kovalevsky, A. Y.; Bagley, K. A.; Coppens, P. *Journal of the American Chemical Society* **2002**, *124*, 9241.

(2) Sheldrick, G. *Acta Crystallogr A* **2008**, *64*, 112.

(3) Cole, J. M.; Boeyens, J. C. A., Ogilvie, J. F., Eds.; Springer Netherlands: 2008, p 29.

(4) McKinnon, J. J.; Spackman, M. A.; Mitchell, A. S. *Acta Crystallographica Section B* **2004**, *60*, 627.